ISSN(Online): 2319-8753
ISSN (Print): 2347-6710

International Journal of Innovative Research in Science, Engineering and Technology

(An ISO 3297: 2007 Certified Organization)

Website: www.ijirset.com

Vol. 6, Issue 8, August 2017

Fuzzy Based Solar PV-Powered SRM Drive for Electric Vehicles

S.Anusha[1], M.Anka Rao[2]

PG Student, Dep. of EEE, JNTU College of Engineering, Ananthapuramu, Andhra Pradesh, India[1]

Assistant Professor, Dep. of EEE, JNTU College of Engineering, Ananthapuramu, Andhra Pradesh, India[2]

ABSTRACT: Hybrid electric vehicle (HEV) technology provides an effective solution for achieving higher fuel economy and better performances with reduced greenhouse gas emissions. For Electric vehicle applications, switched reluctance motor (SRM) is the best suitable one of all the available motors. To increase the driving miles of electric vehicles, a photovoltaic (PV) panel is mounted along with on-board battery bank. A tri-port converter with fuzzy logic controller is proposed to control the energy flow between the PV panel, battery and SRM drive. Six operational modes are presented, four of which are developed for driving modes and rest two for stand still on-board charging. In driving modes, the perturb and observe technique is employed in order to receive maximum power from the PV panel. In stand still charging modes, a grid connected charging topology is developed without any external hardware. A multi section charging control strategy is used for effective utilization of energy in case of battery charging from PV panel directly. The proposed tri-port technology with fuzzy logic controller is developed in MATLAB/SIMULINK environment and the results are proven to be successful in producing reduced harmonic distortion and have the capability to make better market for electric vehicle in the nearby future.

KEYWORDS: Electric Vehicles, Photovoltaic, perturb and observe technique, SRM drive, tri-port converter, fuzzy controller.

I. INTRODUCTION

Electric vehicles have taken a significant leap forward, by advances in motor drives, power converters, batteries and energy management systems. But, due to the limitation of current battery technologies, the driving miles is moderately short that limits the wide utilization of EVs. In terms of motor drives, high performance permanent magnet machines are generally utilized while rare-earth materials are required in large quantities, restricting the wide utilization of EVs. Keeping in mind the end goal to defeat these issues, a photovoltaic panel and a switched reluctance motor (SRM) are introduced to provide power supply and motor drive, respectively.

Firstly, by including the PV panel on top of EV, a sustainable energy source is achieved. Now-a-days, a typical passenger car has a surface enough to install a 250-W PV panel. Second, a SRM needs no rare-earth PMs and is additionally robust so it gets increasing attention in EV applications. While PV panels have low power density for traction drives, they can be used to charge batteries the greater part of the time. For the most part, the PV-fed EV has a comparable structure to the hybrid electrical vehicle, whose internal combustion engine(ICE) is supplanted by the PV panel. The PV-fed EV system is outlined in Fig.1. Its key components include an off-board charging station, a photovoltaic cell, batteries and power converters. In order to decrease the energy conversion processes, one approach is to upgrade the motor to include some on-board charging functions and another solution is based on traditional SRM.

Based on intelligent power modules(IPM), a four-phase half bridge converter is utilized to achieve driving and grid-charging. In spite of the fact that modularization supports mass production, the utilization of half/full bridge topology reduces the system reliability. Paper builds up a basic topology for plug-in hybrid electrical vehicle (HEV) that supports flexible energy flow. In any case for grid charging, the grid should be associated with the generator rectifier that builds the energy conversion process and decreases the charging efficiency. In any case, a powerful topology and control strategy for PV-fed EVs is not yet developed. Since the PV has different characteristics to ICEs, the maximum power point tracking (MPPT) and solar energy utilization are the unique factors for the PV-fed EVs.

ISSN(Online): 2319-8753
ISSN (Print): 2347-6710

International Journal of Innovative Research in Science, Engineering and Technology

(An ISO 3297: 2007 Certified Organization)

Website: www.ijirset.com

Vol. 6, Issue 8, August 2017

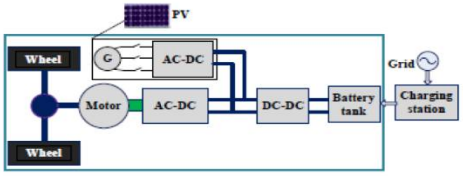

Fig.1: PV-fed hybrid electrical vehicle.

In order to achieve low cost and flexible energy flow modes, a low-cost tri-port converter is proposed in this paper to arrange the PV panel, SRM and battery. Six operational modes are developed to support flexible control of energy flow.

II. TOPOLOGY AND OPERATIONAL MODES

A. Proposed topology and working modes

The proposed tri-port topology has three energy terminals, PV, battery and SRM. They are linked by a power converter which consists of four switching devices (S_0-S_3), four diodes (D_0-D_3) and two relays, as shown in Fig.2.

By controlling relays J1 and J2, the six operation modes are supported which are classified into two major modes as driving mode and charging mode and are sub classified, as shown in Fig.3; the corresponding relay actions are illustrated in Table.1.

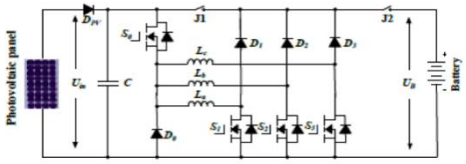

Fig.2: The proposed tri-port topology for PV-powered SRM drive.

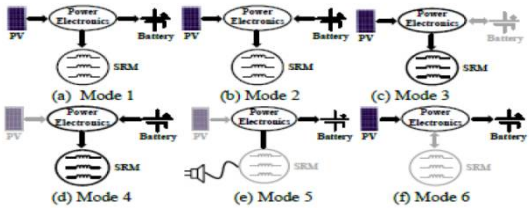

Fig.3: Six operation modes of the proposed tri-port topology

Mode	J1 and J2
1	J1- turn-off ; J2- turn-on
2	J1- turn-on; J2- turn-on
3	J1- turn-on; J2- turn-off
4	J1- turn-on; J2- turn-on
5	J1- turn-on; J2- turn-on
6	J1- turn-off; J2- turn-on

Table.1: J1 and J2 actions under different modes

ISSN(Online): 2319-8753
ISSN (Print): 2347-6710

International Journal of Innovative Research in Science, Engineering and Technology

(An ISO 3297: 2007 Certified Organization)

Website: www.ijirset.com

Vol. 6, Issue 8, August 2017

B. Driving modes

Operating modes 1-4 are the driving modes to provide traction drive to the vehicle.

(1) Mode 1

In mode 1, PV is the energy source to drive the SRM and to charge the battery. At light loads of operation, the energy generated from the PV is more than the SRM needed; the system operates in mode 1. The corresponding operation circuit is shown in Fig.4., in which relay J1 turns off and relay J2 turns on. The PV panel energy feed the energy to SRM and charge the battery; so in this mode, the battery is charged in EV operation condition.

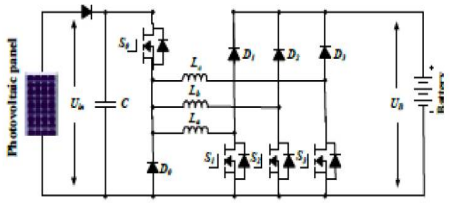

Fig.4: Equivalent circuit under driving condition for mode 1 operation

(2) Mode 2

In mode 2, the PV and battery are both the energy sources to drive the SRM. When the SRM operates in heavy load such as uphill driving or acceleration, both PV panel and battery supply power to SRM. The corresponding operation circuit is shown in Fig.5, in which relay J1 and J2 are turned on.

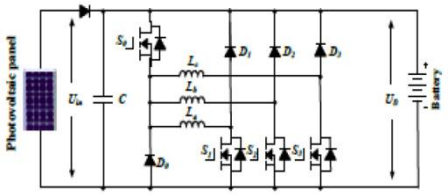

Fig.5: Equivalent circuit under driving condition for mode 2 operation

(3) Mode 3

In mode 3, the PV is the source and battery is idle. When the battery is out of power, the PV panel is the only energy source to drive the vehicle. The corresponding circuit is shown in Fig.6. J1 turns on and J2 turns off.

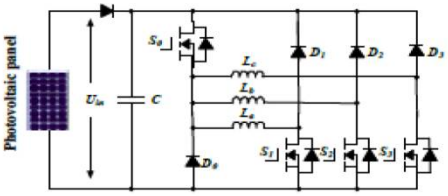

Fig.6: Equivalent circuit under driving condition for mode 3 operation

(4) Mode 4

In mode 4, the battery is the driving source and the PV is idle. When the PV cannot generate electricity due to low solar irradiation, the battery supplies power to the SRM. The corresponding topology is illustrated in Fig.7. In this mode, relays J1 and J2 both are conducting.

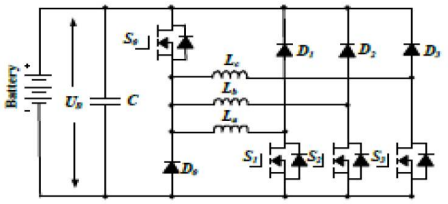

Fig.7: Equivalent circuit under driving condition for mode 4 operation

ISSN(Online): 2319-8753
ISSN (Print): 2347-6710

International Journal of Innovative Research in Science, Engineering and Technology

(An ISO 3297: 2007 Certified Organization)

Website: www.ijirset.com

Vol. 6, Issue 8, August 2017

C.Battery charging modes

Operating modes 5 and 6 are the battery charging modes.

(5) Mode 5

In mode 5, the battery is charged by a single-phase grid while both the PV and SRM are idle. When PV cannot generate electricity, an external power source is needed to charge the battery, such as AC grid. The corresponding circuit is shown in Fig.8. J1 and J2 turns on. Point A is central tapped of phase windings that can be easily achieved without changing the motor structure. One of the three phase windings is split and its mid-point is pulled out, as shown in Fig.8. Phase windings L_{a1} and L_{a2} are employed as input filter inductors. These inductors are part of the drive circuit to form an AC-DC rectifier for grid charging.

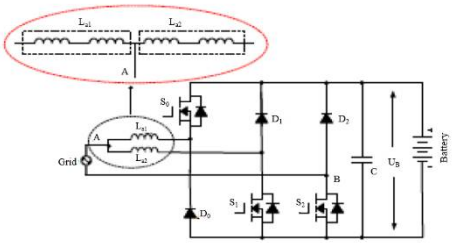

Fig.8: Equivalent circuit under charging condition for mode 5 operation

(6) Mode 6

In mode 6, the battery is charged by the PV and SRM is idle. When the EV is parked under the sun, the PV can charge the battery. J1 turns off; J2 turns on. The corresponding charging circuit is shown in Fig.9.

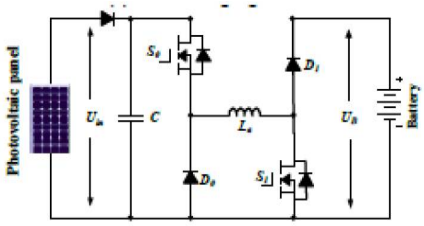

Fig.9: Equivalent circuit under charging condition for mode 6 operation

III.CONTROL STRATEGY UNDER DIFFERENT MODES

In order to make the best use of solar energy for driving the EV, a control strategy under different modes is designed

A. Single source driving mode

As indicated by the distinction in the power sources, there are PV-driving; battery-driving and PV and battery parallel fed sources. In a heavy load condition, the PV power cannot support the EV, mode 2 can be adopted to support enough energy and make full utilization of solar energy. Fig.10(a). demonstrates the equivalent power source; the corresponding PV panel working point is represented in Fig.10(b). Since the PV is paralleled with a battery, the PV panel voltage is clamped to the battery voltage U_B. In mode 2, there are three working states; winding excitation, energy recycling and freewheeling states, as represented in Fig.11. Modes 3 and 4 have comparable working states to mode 2. The difference is that the PV is the only source in mode 3 while the battery is the only source in mode 4.

ISSN(Online): 2319-8753
ISSN (Print): 2347-6710

International Journal of Innovative Research in Science, Engineering and Technology

(An ISO 3297: 2007 Certified Organization)

Website: www.ijirset.com

Vol. 6, Issue 8, August 2017

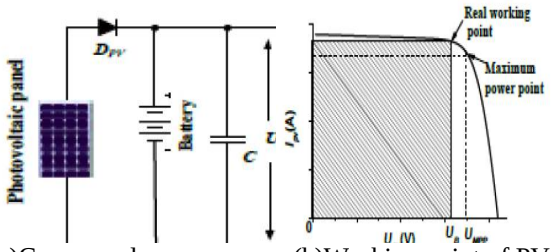

(a)Compound power source (b)Working point of PV

Fig.10: Power supply at mode 2

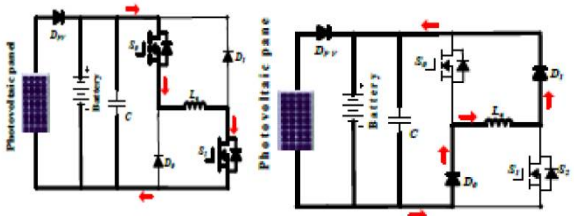

(a)Winding excitation state (b)Energy recycling state

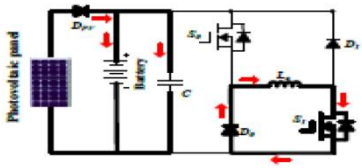

(c)Freewheeling state

Fig.11: Working states at mode 2

Neglecting the voltage drop across the power switches and diodes, the phase voltage is given by

$$U_{in} = R_k i_k + \frac{d\Psi(i_k,\theta_r)}{dt}$$

$$= R_k i_k + L_k\frac{di_k}{dt} + i_k\omega_r\frac{dL_k}{d\theta_r},\ k = a,b,c \quad \ldots\ldots(1)$$

Where U_{in} is the DC- link voltage; k is phase a,b, or c; R_k is the phase resistance; i_k is the phase current; L_k is the phase inductance; θ_r is the rotor position; $\Psi(i_k,\theta_r)$ is the phase flux linkage depending upon the phase current and rotor position and $\omega_r$is the angular speed.

The third term in Eq.1 is the back electromotive force voltage is given by

$$e_k = i_k\omega_r\frac{dL_k}{d\theta_r} \quad \ldots\ldots.(2)$$

Consequently, the phase voltage is found by

$$U_k = R_k i_k + L_k\frac{di_k}{dt} + e_k \ldots\ldots..(3)$$

In the excitation area, turning on S_0 and S_1 will induce a current in phase *a* winding as shown in Fig.11(a). Phase *a*winding is subjected to the positive DC bus voltage.

$$+U_{in} = R_k i_k + L_k\frac{di_k}{dt} + e_k \ldots\ldots.(4)$$

ISSN(Online): 2319-8753
ISSN (Print): 2347-6710

International Journal of Innovative Research in Science, Engineering and Technology

(An ISO 3297: 2007 Certified Organization)

Website: www.ijirset.com

Vol. 6, Issue 8, August 2017

At the point when S_0 is off and S_1 is on, the phase current is in a freewheeling state in a zero voltage loop, as represented in Fig.11(c), the phase voltage is zero.

$$0 = R_k i_k + L_k \frac{di_k}{dt} + e_k \quad \text{.....(5)}$$

In the demagnetization region, S_0 and S_1 are both turned off; whats more, the phase current will flow back to the power supply, as appeared in Fig.11(b). In this state, the phase winding is subjected to the negative DC bus voltage, and the phase voltage is

$$-U_{in} = R_k i_k + L_k \frac{di_k}{dt} + e_k \quad \text{.....(6)}$$

In single source driving mode, the voltage-PWM control is utilized as the fundamental plan as showed in Fig.12. As per the given speed ω^*, the voltage-PWM control is activated at speed control.

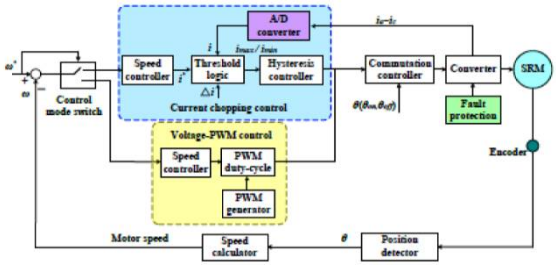

Fig.12: SRM control strategy under single source driving mode.

B. Driving-charging hybrid control strategy

In the driving-charging hybrid control, the PV is the driving source and the battery is charged by the freewheeling current, as represented in drive mode 1. There are two control targets: maximum power point tracking (MPPT) of the PV panel and speed control of the SRM. The dual-source condition is switched from a PV-driving mode. Firstly, the motor speed is controlled at a given speed in mode 3. At that point, J2 is turned on and J1 is turned off to switch to mode 1. By controlling the turn-off point, the maximum power of PV panel can be tracked. There are three steady working states for the double source (mode 1), as shown in Fig.13. In Fig.13(a), S_0 and S_1 conduct, the PV panel charges the SRM winding to drive the motor; In Fig.13(b), S_0 and S_1 turn off; and the battery is charged with freewheeling current of the phase winding. Fig.13(c) represents a freewheeling state.

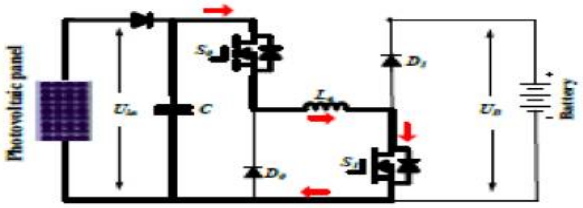

(a) Winding exciting state

ISSN(Online): 2319-8753
ISSN (Print): 2347-6710

International Journal of Innovative Research in Science, Engineering and Technology

(An ISO 3297: 2007 Certified Organization)

Website: www.ijirset.com

Vol. 6, Issue 8, August 2017

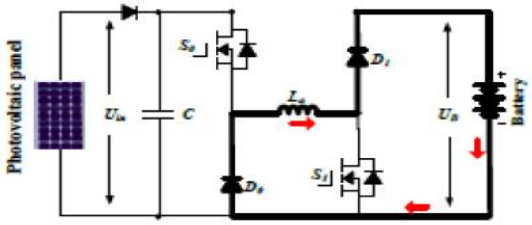

(b) Battery charging state

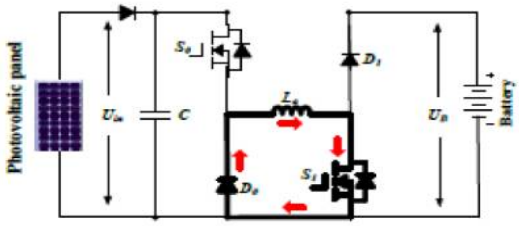

(c) Freewheeling state

Fig.13: Mode 1 working states.

Fig.14 is the control strategy under driving-charging mode. In Fig.14, θ_{on} is the turn on angle of SRM; θ_{off} is the turn-off angle of SRM. By changing turn-on angle, the speed of SRM can be controlled; the maximum power point tracking of PV panel can be achieved by adjusting turn-off angle, which can control the charging current to the battery.

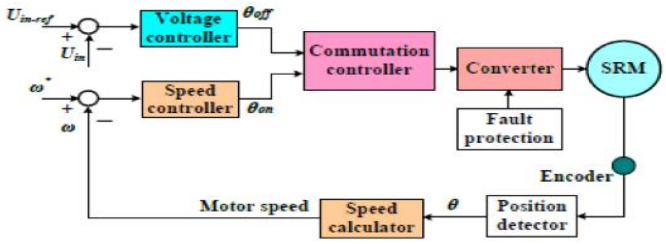

Fig14: Control strategy under driving-charging mode (mode 1)

C.Grid-charging control system

This topology also supports the single-phase grid-charging. There are four basic charging states and S_0 is always turned off. At the point when the grid instantaneous voltage is more than zero, the two working states are exhibited in Fig.15(a) and (b). In Fig.15(a), S_1 and S_2 conduct, the grid voltage charges the phase winding L_{a2}, the relating condition can be communicated as Eq.7; In Fig.15(b), S_1 turns off and S_2 conducts, the grid is associated in series with phase winding to charge the battery, the related condition can be given as Eq.8.

$$U_{grid} = L_{a2} . \frac{di_{grid}}{dt} \quad ....(7)$$

$$U_B - U_{grid} = L_{a2} . \frac{di_{grid}}{dt} \quad .....(8)$$

At the point when the grid instantaneous voltage is below zero, the two working states are introduced in Fig.15(c) and (d). In Fig.15(c), S_1 and S_2 conduct, the grid voltage charges the phase winding L_{a1} and L_{a2}, the comparing condition

ISSN(Online): 2319-8753
ISSN (Print): 2347-6710

International Journal of Innovative Research in Science, Engineering and Technology

(An ISO 3297: 2007 Certified Organization)

Website: www.ijirset.com

Vol. 6, Issue 8, August 2017

can be represented in Eq.9; In Fig. 15(d), S_1 continues conducting and S_2 turns off, the grid is associated in series with phase winding L_{a1} and L_{a2} to charge the battery, the related condition can be represented as in Eq.10.

$$U_{grid} = \frac{L_{a1}+L_{a2}}{L_{a1}.L_{a2}} \cdot \frac{di_{grid}}{dt} \quad \text{.....(9)}$$

$$-U_B - U_{grid} = \frac{L_{a1}+L_{a2}}{L_{a1}.L_{a2}} \cdot \frac{di_{grid}}{dt} \quad \text{.....(10)}$$

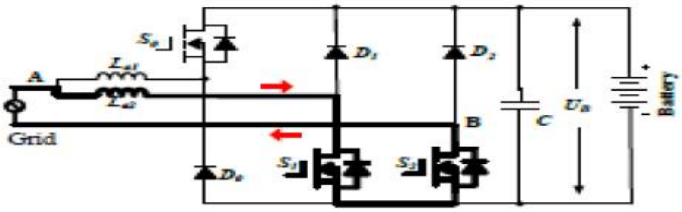

(a) Grid charging state 1 (U_{grid}> 0)

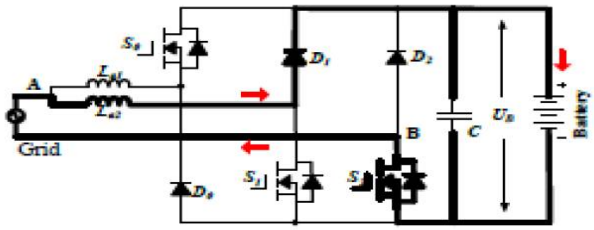

(b) Grid charging state 2 (U_{grid}> 0)

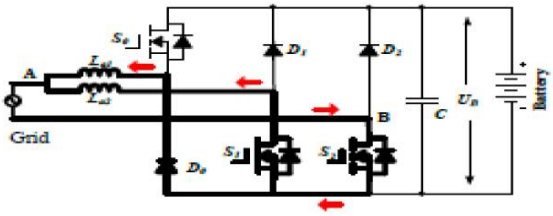

(c) Grid charging state 3 (U_{grid}< 0)

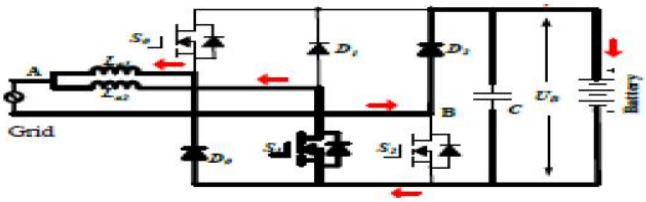

(d) Grid charging state 4 (U_{grid}< 0)

Fig.15: Mode 5 charging states.

ISSN(Online): 2319-8753
ISSN (Print): 2347-6710

International Journal of Innovative Research in Science, Engineering and Technology

(An ISO 3297: 2007 Certified Organization)

Website: www.ijirset.com

Vol. 6, Issue 8, August 2017

In Fig.16, U_{grid} is the grid voltage; by the phase locked loop (PLL), the phase data can be got; I_{ref_grid} is the given amplitude of the grid current. Combining sinθ and I_{ref_grid}, the instantaneous grid current i_{ref_grid} can be figured. In this mode, when $U_{grid}>0$, the inductance is L_{a2}; when $U_{grid}<0$, the inductance is paralleled L_{a1} and L_{a2}; so in order to adopt the change in the inductance, hysteresis control is employed to acknowledge grid current regulation. Besides, hysteresis control has great loop performance, global stability and small phase lag that makes grid connected control stable.

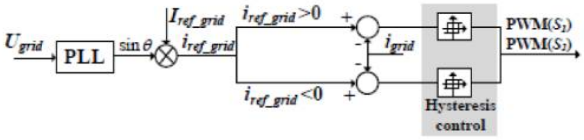

Fig.16: Grid-connected charging control (Mode 5)

D. PV-fed charging control system

In this mode, the PV panel charges the battery specifically by the driving topology. The phase windings are employed as inductor; driving topology can be worked as interleaved Buck boost charging topology. For one phase, there are two states, as appeared in Fig.17(a) and (b). Whenever S_0 and S_1 turn on, the PV panel charges phase inductance; when S_0 and S_1 turns off, the phase inductance discharges energy to battery. According to the state-of-charging (SoC), there are three stages to make full utilize of solar energy and keep the battery in healthy condition, as represented in Fig.17(c). During stage 1, the battery is in extremely lack energy condition (i.e., from 0 ~ SoC) , the MPPT control strategy is employed to make full use of solar energy. During stage 2, the corresponding battery SoC is in SoC_1~SoC_2, the constant voltage control is adapted to charge the battery. During stage 3, the corresponding battery SoC is in SoC2~1, the micro current charging is adapted. In order to simplify the control strategy, constant voltage is employed in PV panel MPPT control.

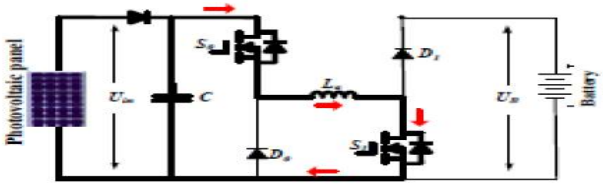

(a) Phase inductance charging

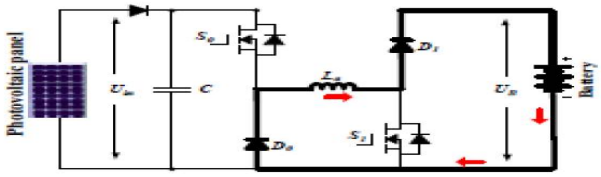

(b) Battery charging

ISSN(Online): 2319-8753
ISSN (Print): 2347-6710

International Journal of Innovative Research in Science, Engineering and Technology

(An ISO 3297: 2007 Certified Organization)

Website: www.ijirset.com

Vol. 6, Issue 8, August 2017

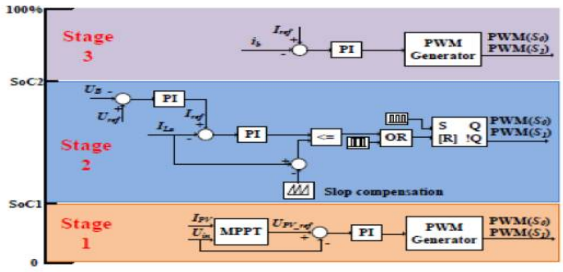

(c) Charging control strategy

Fig.17: Mode 6 charging states and control strategy

V. FUZZY LOGIC CONTROLLER

In this section, we will illustrate the principles of fuzzy controllers, their design and their use in electric vehicles. The principle of fuzzy logic controllers is based on the techniques of artificial intelligence whose theoretical foundations have been made by Zedeh. The fuzzy logic controller operates in knowledge based way, and its knowledge relies on a set of linguistic if….then rules, like human operator. The block diagram of fuzzy logic control is mainly depicted in.

The FLC is made up of parameters such as rules base, database, membership functions, input and output scaling factor. Fig.18 represents the block diagram of fuzzy logic controller. The main parts of block diagram are fuzzification, defuzzification, inferace and database.

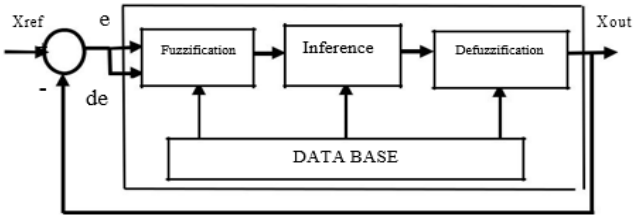

Fig.18: Fuzzy logic controller

Concerning the definition of membership function, the controllers has two inputs (e(k), ce(k)) and a single output. Fig.19, Fig.20 and Fig.21 show respectively the membership functions of inputs and output variables.

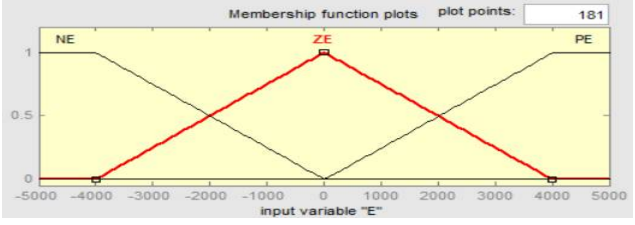

Fig.19: Input membership function of “e”

ISSN(Online): 2319-8753
ISSN (Print): 2347-6710

International Journal of Innovative Research in Science, Engineering and Technology

(An ISO 3297: 2007 Certified Organization)

Website: www.ijirset.com

Vol. 6, Issue 8, August 2017

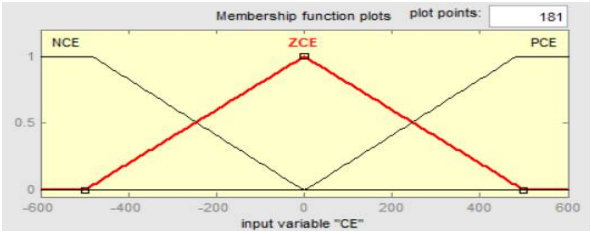

Fig.20: Input membership function of “ce”

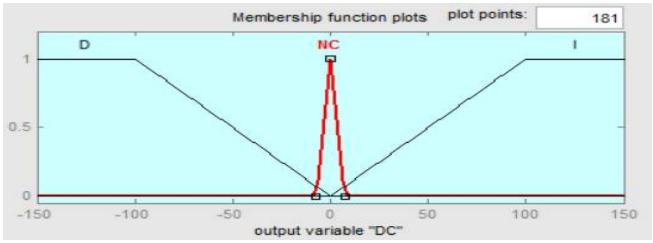

Fig.21: Output membership function of “dc”

The number of linguistic value are characterized by the symbols likewise; NB: Negative error, ZE: Zero error, PE: Positive error, NCE: Negative change in error, ZCE: Zero change in error, PCE: Positive change in error, NC: No change.

The development of the basic rules of the controller is interrupted by the rules of the form (if..then). The fuzzy rules that defined the output of the controllers according to inputs. Where Table 2 present two linguistics variables of inputs “e” and its variation “ce” and the output variable “dc”.

CE / E	NCE	ZCE	PCE
NE	D	D	D
ZE	D	NC	I
PE	I	I	I

Table.2: Rule base for fuzzy control

IV. SIMULATION

A 12/8 SRM is initially modeled in MATLAB/Simulink utilizing parameters in Table 3. Fig.22(a) presents the simulation results at mode 1. The load torque is set as 35 Nm, the PV panel voltage is controlled at the maximum power point. The freewheeling current is used to charge the battery. Fig.22(b) demonstrates the simulation results of the single-source driving modes (mode 2-4).

Parameter	Value
SRM	12/8
PV panel	
Maximum power point voltage reference voltage	310 V
Battery voltage	350 V
Constant voltage control reference voltage	355 V
Constant current control reference current	1 A
Mode 1, charging current	60 A
Mode 4, driving speed	1250 rpm
Mode 6, constant voltage charging reference	355 V
Mode 6, constant current charging reference	1 A

Table.3: Simulation parameters

ISSN(Online): 2319-8753
ISSN (Print): 2347-6710

International Journal of Innovative Research in Science, Engineering and Technology

(An ISO 3297: 2007 Certified Organization)

Website: www.ijirset.com

Vol. 6, Issue 8, August 2017

Fig.23 demonstrates the simulation results of charging where Fig.23(a) is for grid-charging. The positive half current quality is superior to anything the negative half that is caused by the change in the grid-connected inductance. Fig.23(b) and (c) are for PV-charging. Fig.23(b) presents the step change from stage 1 to 2. In stage 1, the battery is low in SoC. In order to achieve MPPT of the PV, the constant voltage control is utilized and the PV output voltage is controlled at maximum power point (310 V), as appeared in Fig.23(b). In stage 2, a constant voltage is embraced; the reference voltage is set to 355 V. As appeared in Fig.23(b), the charging converter output voltage is controlled at reference voltage in the step change from stage 1 to stage 2. In stage 3, 1A trickle charging is moreover accomplished, as appeared in Fig.23(c).

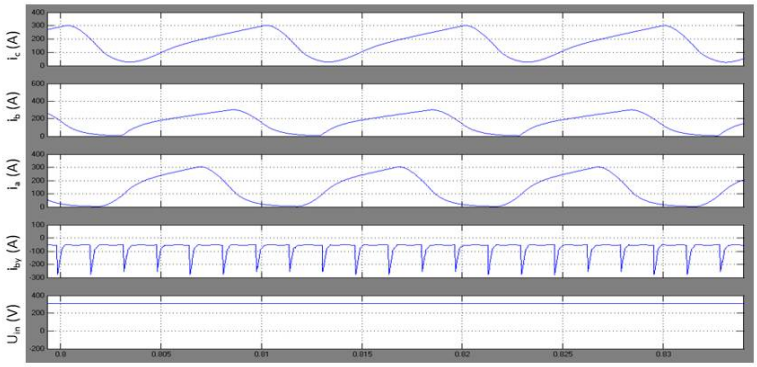

Fig.22(a): Simulation results of driving-charging mode (mode 1)

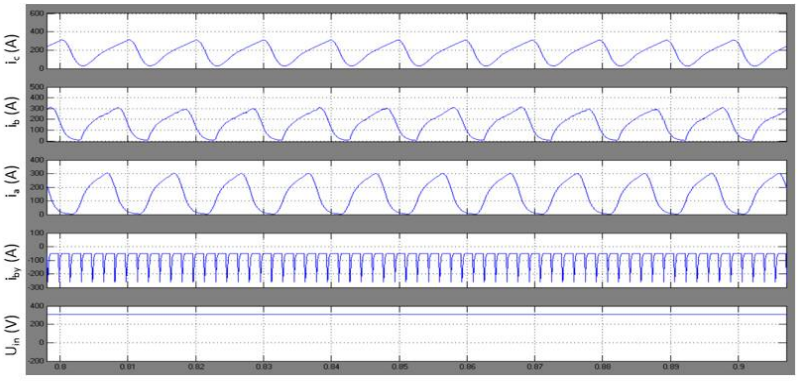

Fig.22(b): Simulation results of driving-charging mode (mode 2)

ISSN(Online): 2319-8753
ISSN (Print): 2347-6710

International Journal of Innovative Research in Science, Engineering and Technology

(An ISO 3297: 2007 Certified Organization)

Website: www.ijirset.com

Vol. 6, Issue 8, August 2017

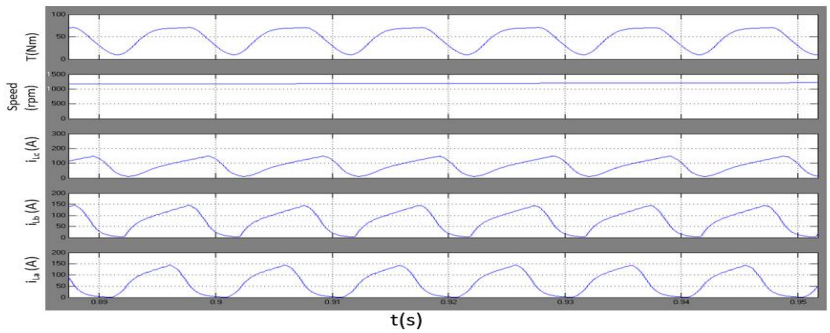

Fig.22(c): Simulation results of single source driving mode (modes 3 and 4)
Fig.22: Simulation results for driving conditions at modes 1,3 and 4.

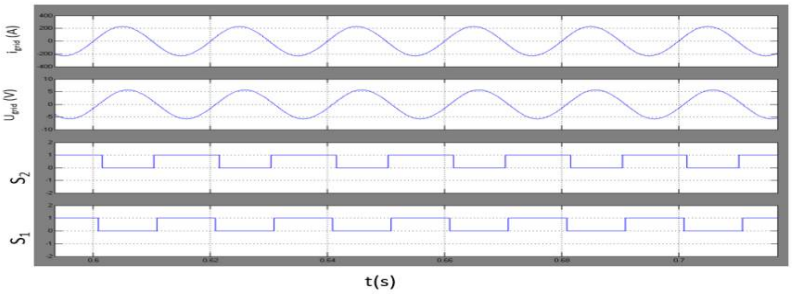

Fig.23(a): Grid charging (mode 5)

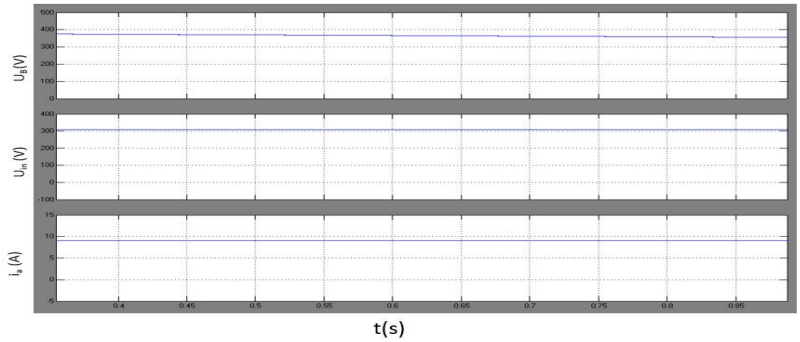

Fig.23(b): PV charging mode 6 (stage 1 to stage 2)

ISSN(Online): 2319-8753
ISSN (Print): 2347-6710

International Journal of Innovative Research in Science, Engineering and Technology

(An ISO 3297: 2007 Certified Organization)

Website: www.ijirset.com

Vol. 6, Issue 8, August 2017

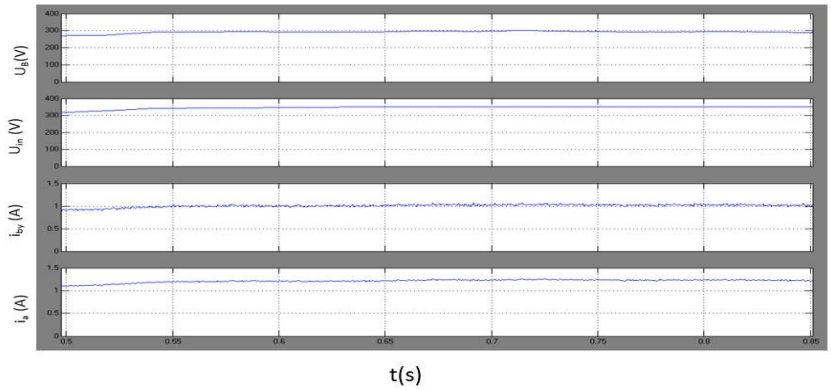

Fig.23(c): PV charging mode 6 (stage 2 to stage 3)
Fig.23: Simulation results for charging modes.

THD in % using PI controller:	THD in % using fuzzy controller:
Mode 1: I_a =41.43, I_b =38.12, I_c =64.58	Mode 1: I_a =25.72, I_b =19.82, I_c =27.17
Mode 2: I_a =43, I_b =31.01, I_c =71.52	Mode 2: I_a =25.29, I_b =14.46, I_c =27.94
Mode 3: I_{La}=82.66,I_{Lb}=33.68,I_{Lc}=43.47	Mode 3: I_{La}=51.25,I_{Lb}=17.51,I_{Lc}=18.26
Mode 4: I_{La}=64.68,I_{Lb}=34.25,I_{Lc}=41.87	Mode 4: I_{La}=40.1,I_{Lb}=17.51,I_{Lc}=17.56
Mode 5: U_{grid} = 0.004535, I_{grid} = 0.004864	Mode 5: U_{grid} = 0.004535, I_{grid} = 0.004864
Mode 6: stage 1 I_a = 11.5	Mode 6: stage 1 I_a = 5.982
Mode 6: stage 2 I_{La} = 2.377	Mode 6: stage 2 I_{La} = 0.9965
Mode 6: stage 3 I_a = 2.429, I_b = 2.632	Mode 6: stage 3 I_a = 1.815, I_b = 1.969

Table.4: THD values using PI controller and fuzzy logic method.

VI. CONCLUSION

As PV-fed electric vehicles are greener and has more sustainable technology than conventional IC engine vehicles, this work will provide a feasible solution to reducing the total costs and CO_2 emissions of electrified vehicles. In order to tackle the range anxiety of using electric vehicles and decrease the system cost, a combination of the PV panel and SRM is proposed as the EV driving system. Fuzzy logic controller is used in place of PI controller in order to reduce total harmonic distortions and can be observed that with use of fuzzy logic controller THD has decreased almost to half than when PI controller is used.

ISSN(Online): 2319-8753
ISSN (Print): 2347-6710

International Journal of Innovative Research in Science, Engineering and Technology

(An ISO 3297: 2007 Certified Organization)

Website: www.ijirset.com

Vol. 6, Issue 8, August 2017

The main contributions of this paper are:
(i)A tri-port converter with fuzzy logic controller is used to control the energy flow between the PV panel, battery and SRM drive.
(ii)Six working modes are developed to achieve flexible energy flow for driving control, driving/charging hybrid control and charging control.
(iii)A novel grid-charging topology is formed without a need for external power electronic devices.
(iv)Fuzzy logic controller is used instead of PI controller to reduce total harmonic distortion.
(v)A PV-fed battery charging control scheme is developed to improve the solar energy utilization.

In this paper, we introduced fuzzy logic controller in place of PI controller and observed the improved performance of vehicle with reduced harmonic distortions. A tri port converter is proposed in this paper to control the energy flow between the PV panel, battery and SRM. Furthermore, the proposed technology may also be applied to similar applications such as fuel cell powered EVs instead of batteries. As fuel cells have much higher power density and are thus better suited for EV applications.

REFERENCES

[1] A. Emadi, L. Young-Joo, K. Rajashekara, "Power electronics and motor drives in electric, hybrid electric, and plug-in hybrid electric vehicles," IEEE Trans. Ind. Electron., vol. 55, no. 6, pp. 2237-2245, Jun. 2008.
[2] B. l. K. Bose, "Global energy scenario and impact of power electronics in 21st century," IEEE Trans. Ind. Electron., vol. 60, no. 7, pp. 2638-2651, Jul. 2013.
[3] J. de Santiago, H. Bernhoff, B. Ekergård, S. Eriksson, S. Ferhatovic, R. Waters, and M. Leijon,"Electrical motor drivelines in commercial all-electric vehicles: a review," IEEE Trans. Veh. Technol., vol. 61, no. 2, pp. 475-484, Feb. 2012.
[4] Z. Amjadi, S. S. Williamson, "Power-electronics-based solutions for plug-in hybrid electric vehicle energy storage and management systems," IEEE Trans. Ind. Electron., vol. 57, no. 2, pp. 608-616, Feb. 2010.
[5] A. Kuperman, U. Levy, J. Goren, A. Zafransky, and A. Savernin, "Battery charger for electric vehicle traction battery switch station," IEEE Trans. Ind. Electron., vol. 60, no. 12, pp. 5391-5399, Dec. 2013.
[6]S.Madhusudhanan,N.K.Mohanty,"Simulation of fuzzy and PI control of asymmetric bridge converter fed switched reluctance motor drive," IJCTA, 9(13), pp.6047-6056, 2016.
[7]S.Prabhu, A.Sakul Hameed, Dr.M.Satish Kumar, "Control of switched reluctance motor using dynamic braking," IJES,vol.3, pp.2319-1805, 2014.
[8]S.Dhatchayani, B.Barathy, A.Kavitha, "Development of buck switch mode rectifier charger for battery powered switched reluctance motor drive," IJAREEIE,vol. 3, pp:2278-8875, April 2014.
[9]G.Divya, Ramani Kalpathi, "Regenerative braking using switched reluctance generator," IJSER, vol.5, pp.2229-5518, April-2014.